

Article

Chaos Game Optimization-Hybridized Artificial Neural Network for Predicting Blast-Induced Ground Vibration

Shugang Zhao, Liguan Wang and Mingyu Cao *

School of Resources and Safety Engineering, Central South University, Changsha 410083, China; 185502032@csu.edu.cn (S.Z.); liguan_wang@csu.edu.cn (L.W.)

* Correspondence: 215502037@csu.edu.cn

Abstract: In this study, we introduced the chaos game optimization-artificial neural network (CGO-ANN) model as a novel approach for predicting peak particle velocity (PPV) induced by mine blasting. The CGO-ANN model is compared with other established methods, including the particle swarm optimization-artificial neural network (PSO-ANN), the genetic algorithm-artificial neural network (GA-ANN), single ANN, and the USBM empirical model. The aim is to demonstrate the superiority of the CGO-ANN model for PPV prediction. Utilizing a dataset comprising 180 blasting events from the Tonglushan Copper Mine in China, we investigated the performance of each model. The results showed that the CGO-ANN model outperforms other models in terms of prediction accuracy and robustness. This study highlights the effectiveness of the CGO-ANN model as a promising tool for PPV prediction in mining operations, contributing to safer and more efficient blasting practices.

Keywords: peak particle velocity (PPV); chaos game optimization (CGO); artificial neural network (ANN); mine blasting; prediction model; Tonglushan Copper Mine



Citation: Zhao, S.; Wang, L.; Cao, M. Chaos Game Optimization-Hybridized Artificial Neural Network for Predicting Blast-Induced Ground Vibration. *Appl. Sci.* **2024**, *14*, 3759. <https://doi.org/10.3390/app14093759>

Academic Editor: Ricardo Castedo

Received: 27 March 2024

Revised: 21 April 2024

Accepted: 24 April 2024

Published: 28 April 2024



Copyright: © 2024 by the authors. Licensee MDPI, Basel, Switzerland. This article is an open access article distributed under the terms and conditions of the Creative Commons Attribution (CC BY) license (<https://creativecommons.org/licenses/by/4.0/>).

1. Introduction

Blasting serves as a fundamental technique for rock breakage in both mining and civil engineering ventures worldwide, owing to its efficiency and cost-effectiveness compared to alternative methods. It enables the successful completion of various large-scale projects, rendering them technically and economically feasible [1]. Despite its effectiveness, blasting operations release only a fraction of the explosive energy towards actual rock breakage and displacement, with the remaining energy contributing to undesirable environmental effects such as ground vibration, noise, fly rock, and noxious gases [2,3]. These repercussions can extend to reserved slopes and structures, potentially compromising their structural integrity.

Among the detrimental effects of blasting, ground vibration stands out as a major concern for mine planners, designers, and environmentalists [3,4]. Ground vibration manifests as a wave motion, propagating outward from the blasting source akin to ripples spreading across a water surface after an object impact. Peak particle velocity (PPV) serves as the primary parameter for evaluating blast-induced ground vibration, according to regulations governing blasting practices and research on blast-induced ground vibration [5]. The archived surveys and obtained results demonstrated that PPV can cause structural damage to buildings, bridges, and other infrastructure in the vicinity; disturb sensitive ecosystems, such as nearby wildlife habitats or aquatic environments; cause settlement or subsidence of the ground, particularly in areas with loose or uncompacted soil; disturb underground aquifers or disrupt nearby water bodies, leading to contamination from pollutants or sedimentation; and promote rockburst in deep openings [6–11].

Efforts to quantify blast-induced ground vibration based on PPV have resulted in three main categories: field measurement, empirical equations, and computational methods (including finite element and artificial intelligence techniques). While field measurements

offer accuracy, they are costly, time-consuming, and site-specific, leading engineers to rely predominantly on traditional empirical models.

Several researchers have proposed variants of traditional empirical models, such as those by Thoenen et al. [12], Langefors and Kihlström [13], Ambraseys and Hendron [14], and others [15,16]. Traditional empirical models have paved the way for intelligent algorithmic predictions, with recent studies showcasing the efficacy of techniques like modified Kuz–Ram models and comparisons between empirical formulations and intelligent algorithms [17]. However, these equations, while simple to implement, are known to be inaccurate and site-specific, rendering them unusable for rocks with similar characteristics to those used in developing the equations.

Over the years, researchers have sought to overcome the limitations of conventional empirical equations by employing advanced soft computing analytics to describe complex real-world phenomena. Techniques such as artificial neural networks (ANNs), fuzzy models, linear regression, decision trees, random forests, and deep learning have been utilized to predict and estimate blast-induced vibrations [18–25]. Notable studies by Refs. [23–25] have focused on predicting ground vibration induced by blasting using ANN methodologies, categorizing their models based on the parameters employed. Additionally, research has explored various machine learning (ML) approaches, with ANNs, support vector machines (SVMs), and adaptive neuro-fuzzy inference systems (ANFIS) emerging as prominent algorithms [18]. Hybrid models combining multiple ML algorithms have shown promise in enhancing prediction accuracy, although they often present complex mathematical formulations [18,26].

In open-pit mining, there is an increasing trend towards using intelligent algorithms for predictive and optimization techniques to address blast-induced ground vibration. As a result, researchers have suggested integrating intelligent algorithms and additional influencing factors into prediction models to improve accuracy [27–29]. Recent endeavors have concentrated on enhancing prediction models through hybrid approaches like cuckoo optimization and particle swarm algorithms, resulting in better PPV predictions [30–32]. Moreover, preprocessing input data using methods such as clustering and feature selection has demonstrated potential in boosting model performance [33–35].

Metaheuristic algorithms play a vital role in optimizing hybrid models for blast vibration prediction and mine-blasting optimization [30–32,36–38]. For instance, the grey wolf optimization (GWO), hunger games search (HGS), manta ray foraging optimization (MRFO), aquila optimization (AO), the bat-inspired algorithm (BA), and the naked mole-rat algorithm (NMRA) have been utilized to predict blast-induced ground vibration [36,39] under the integration of ANN models, while the whale optimization algorithm (WOA), grey wolf optimization (GWO), and Bayesian optimization algorithm (BO) have been applied to effectively optimize the hyper-parameters of the XGBoost model for predicting blast-induced ground vibration [40]. Chen et al. [41] also utilized various metaheuristic algorithms to optimize another machine learning model (i.e., SVR), such as the firefly algorithm (FA), the genetic algorithm (GA), and particle swarm optimization (PSO).

Existing methodologies, such as empirical equations and traditional prediction models, often lack the accuracy and flexibility required to effectively capture the complex dynamics of blast-induced ground vibrations. While some studies have attempted to address this by employing advanced soft computing techniques like artificial neural networks (ANNs) and machine learning algorithms, many still fall short in achieving optimal prediction accuracy. Additionally, some models may provide impractical mathematical formulations or require significant manual tuning, making them less suitable for real-world applications.

In light of these limitations, there is a pressing demand for a novel and robust predictive model capable of accurately forecasting PPV while circumventing the constraints of current methodologies. Thus, this study introduces a pioneering chaos game optimization (CGO)-ANN model, which integrates CGO, a metaheuristic optimization technique, with the ANN model. This hybrid approach capitalizes on the advantages of both methodologies, employing CGO to optimize the parameters of the ANN model and enhance its predictive

efficacy. Furthermore, the PSO and GA algorithms were employed to optimize the ANN model, and a comparison was made between the CGO-ANN model, a single ANN, and USBM empirical models in PPV prediction. By introducing the CGO-ANN model, this study seeks to rectify the limitations of prior approaches and offer a more precise and dependable tool for PPV prediction in mine blasting scenarios. Through rigorous testing and validation, the proposed CGO-ANN model endeavors to demonstrate its superiority over existing methodologies, providing enhanced predictive accuracy and practical utility in real-world mining contexts.

2. Methodology

2.1. Artificial Neural Network

The principle of ANNs is grounded in simulating the structure and functions of the human brain to process information. ANNs belong to the domain of artificial intelligence, alongside other methods such as case-based reasoning, expert systems, and genetic algorithms. While classical statistics, fuzzy logic, and chaos theory comprise related fields, ANNs stand out for their ability to perform massively parallel computation for data processing and knowledge representation.

At its core, an ANN comprises interconnected processing elements known as neurons, organized into distinct layers within the network structure. The most effective type of ANN, the multi-layer perceptron (MLP), typically consists of three layers: an input layer, an output layer, and one or more hidden layers. Neurons within each layer are interconnected but not within the same layer. Information processing occurs as signals are transmitted between neurons through connection links, each with an associated weight that modulates the signal. The sum of weighted input signals to each neuron is transformed by an activation function, typically nonlinear in nature.

The performance of an ANN is influenced by the network architecture, the activation function, and the learning algorithm. For network architecture, this involves the arrangement of neurons and layers within the network. The number of hidden layers and neurons is determined by the complexity of the problem being addressed. In addition, the activation function determines how the weighted sum of inputs is transformed into an output signal. It introduces nonlinearity into the network, allowing it to model complex relationships between inputs and outputs. The learning algorithm governs how the network adjusts its connection weights during training to minimize prediction errors. One commonly used algorithm is the feedforward backpropagation algorithm, which updates weights based on the difference between the predicted and actual outputs.

During training, the network is exposed to a sufficient number of input-output patterns, known as training pairs, to learn the underlying relationships between inputs and outputs. The training process involves iteratively adjusting the connection weights until a specified error goal, such as root mean square error (RMSE), is reached. Once trained, the network can be used to predict outputs (e.g., blast-induced ground vibration) for new input data. Figure 1 illustrates an ANN model for predicting blast-induced ground vibration.

2.2. Chaos Game Optimization

The chaos game optimization (CGO) algorithm, introduced by Talatahari and Azizi [42], is an innovative metaheuristic optimization technique rooted in chaos theory and fractals. Chaos theory, a branch of mathematics, explores the behavior of dynamic systems highly sensitive to initial conditions, revealing hidden patterns and definite rules amidst apparent randomness [43–45]. It emphasizes interconnections, feedback loops, self-similarity, and self-organization in complex systems, epitomized by the butterfly effect, where small changes can lead to significant outcomes elsewhere.

Fractals, geometric structures with self-similarity at various scales, play a central role in chaos theory. The Sierpiński fractal, an equilateral triangle recursively subdivided into smaller triangles, exemplifies self-similarity. CGO leverages chaos theory and fractals to optimize solutions.

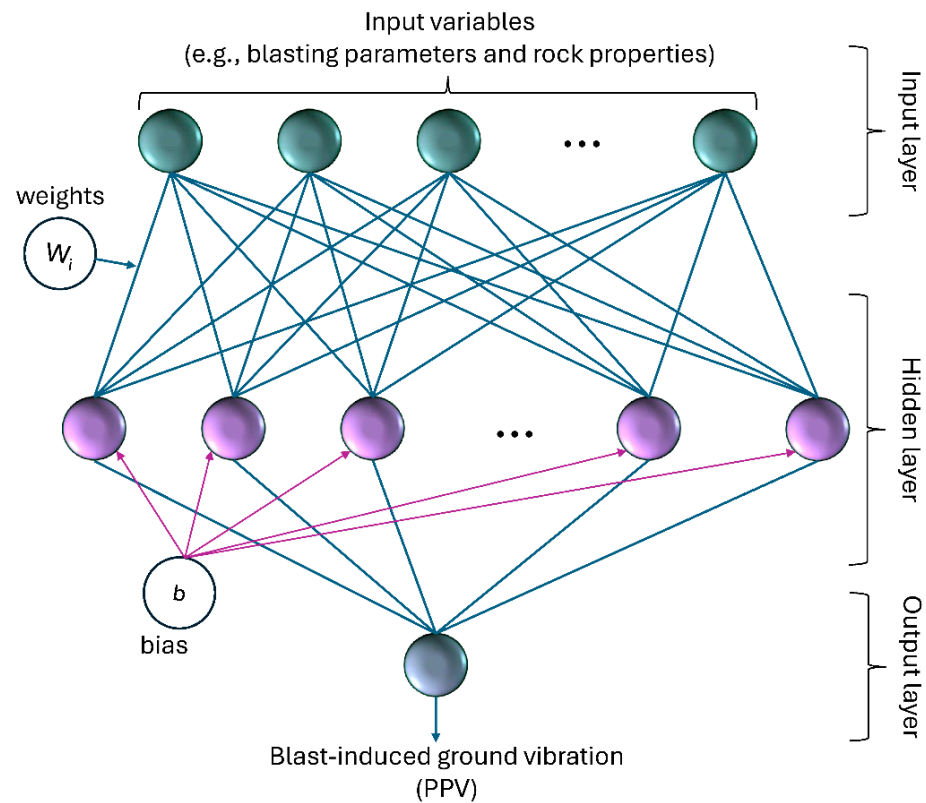


Figure 1. ANN framework for predicting blast-induced ground vibration.

In the chaos game methodology, initially, three vertices are chosen to form a triangle, each marked with a different color. A random initial point, or seed, is selected within the triangle. Rolling a die with colored faces determines the movement of the seed towards the corresponding vertex, halving the distance. This process iterates, with the new seed position becoming the starting point for subsequent iterations. Through repeated die rolls, the seed converges towards creating the Sierpiński triangle fractal.

The CGO algorithm inherits chaos theory’s emphasis on sensitivity to initial conditions, utilizing fractal generation principles to iteratively optimize solutions. By integrating chaos game theory into optimization, CGO offers a parameter-free approach, distinguishing it from conventional optimization methods. This unique blend of chaos theory, fractals, and optimization makes CGO a promising tool for tackling complex optimization problems.

The mathematical formulation of CGO draws upon the self-similarity principles inherent in chaos theory and the fundamental techniques for generating the Sierpiński triangle, and it is described as follows:

Initially, an initialization procedure is established by defining the initial positions (X_i) of solution candidates within the predetermined search space, which is modeled as a Sierpiński triangle:

$$X = \begin{bmatrix} X_1 \\ X_2 \\ \vdots \\ X_i \\ \vdots \\ X_n \end{bmatrix} = \begin{bmatrix} x_1^1 x_1^2 \cdots x_1^j \cdots x_1^d \\ x_2^1 x_2^2 \cdots x_2^j \cdots x_2^d \\ \cdots \\ x_i^1 x_i^2 \cdots x_i^j \cdots x_i^d \\ \cdots \\ x_n^1 x_n^2 \cdots x_n^j \cdots x_n^d \end{bmatrix}, \begin{cases} i = 1, 2, \dots, n \\ j = 1, 2, \dots, d \end{cases} \quad (1)$$

$$x_i^j(0) = x_{i,\min}^j + rand(x_{i,\max}^j - x_{i,\min}^j), \begin{cases} i = 1, 2, \dots, n \\ j = 1, 2, \dots, d \end{cases} \quad (2)$$

where the problem dimension and the total number of initialized candidates within the Sierpiński triangle search space are denoted by d and n , respectively. $x_i^j(0)$ represents the initial value of the j th design variable for the i th point in the search space, with $x_{i,\min}^j$ and $x_{i,\max}^j$ indicating the lower and upper bounds of the decision variables. The variable $Rand$ denotes a randomly generated number within the range $[0, 1]$.

The primary search loop of the CGO algorithm involves adjusting the initially created points to achieve the complete shape of a Sierpiński triangle. Each point within the triangle is connected to two other points to form a temporary triangle: the Global Best GB vector, representing the best solution found so far, and the Mean Group MG_i , obtained by averaging a set of points randomly selected around the candidate solution (i th point).

To update the position of each temporary triangle, three individual seeds are placed at the triangle's three points. For the seed located at the i th candidate point X_i , a die with three red and three green faces is used. If the green face appears upon rolling the die, the seed moves towards the global best solution GB ; if the red face appears, it moves towards the i th mean group MG_i . This process is mathematically represented by generating two random integers between 0 and 1, with the possibility of generating two equal integers taken into account, allowing the seed to move along the line connecting GB and MG_i . This aspect is illustrated in Figure 2a, with its mathematical representation provided in Equation (3).

$$Seed_i^1 = X_i + \alpha_i \times (\beta_i \times GB - \gamma_i \times MG_i), i = 1, 2, \dots, n \quad (3)$$

where $Seed_i^1$ represents the seed positioned at the i th solution candidate point; α_i denotes the movement limitation factor; β_i and γ_i are vectors containing randomly generated numbers within the range $[0, 1]$.

For the seed positioned at the global best solution point GB , a die with three red and three blue faces is used. Upon rolling the die, if a blue face appears, the seed moves towards the i th candidate X_i ; if a red face appears, it moves towards the i th mean group MG_i . Considering the possibility of generating two equal integers, the seed can also move along the line connecting X_i and MG_i . This concept is illustrated in Figure 2b, while the mathematical representation is shown in Equation (4).

$$Seed_i^2 = GB + \alpha_i \times (\beta_i \times X_i - \gamma_i \times MG_i), i = 1, 2, \dots, n \quad (4)$$

where $Seed_i^2$ represents the seed positioned at the global best point GB .

To adjust the seed located at the mean group point MG_i , a die with three blue and three green faces is employed. Upon rolling the die, if the blue face appears, the seed moves towards the i th candidate X_i ; if the green face appears, it moves towards the global best GB . Accounting for the potential occurrence of two equal integers, the seed may also traverse the line connecting X_i and GB . This concept is illustrated in Figure 2c, with its mathematical representation provided in Equation (5).

$$Seed_i^3 = MG_i + \alpha_i \times (\beta_i \times X_i - \gamma_i \times GB), i = 1, 2, \dots, n \quad (5)$$

To improve the mutation phase of the CGO, a fourth seed positioned at the i th candidate point X_i is introduced for position updating. This seed is allowed to move freely and randomly within the search space. This concept is illustrated in Figure 2d, with the mathematical representation shown in Equation (6).

$$Seed_i^4 = X_i \left(x_i^k = x_i^k + \delta \right), k = 1, 2, \dots, d \quad (6)$$

where δ is a vector with random number in the range of 0 and 1.

The movement limitation factor α_i is intricately integrated into the position updating process to regulate the exploration and exploitation rates of the CGO. This factor is randomly determined by selecting one of the following scenarios:

$$\alpha_i = \begin{cases} Rand \\ 2 \times Rand \\ (\rho \times Rand) + 1 \\ (\varepsilon \times Rand) + \varepsilon \end{cases} \quad (7)$$

where ρ and ε are two random integers in the range of [0, 1].

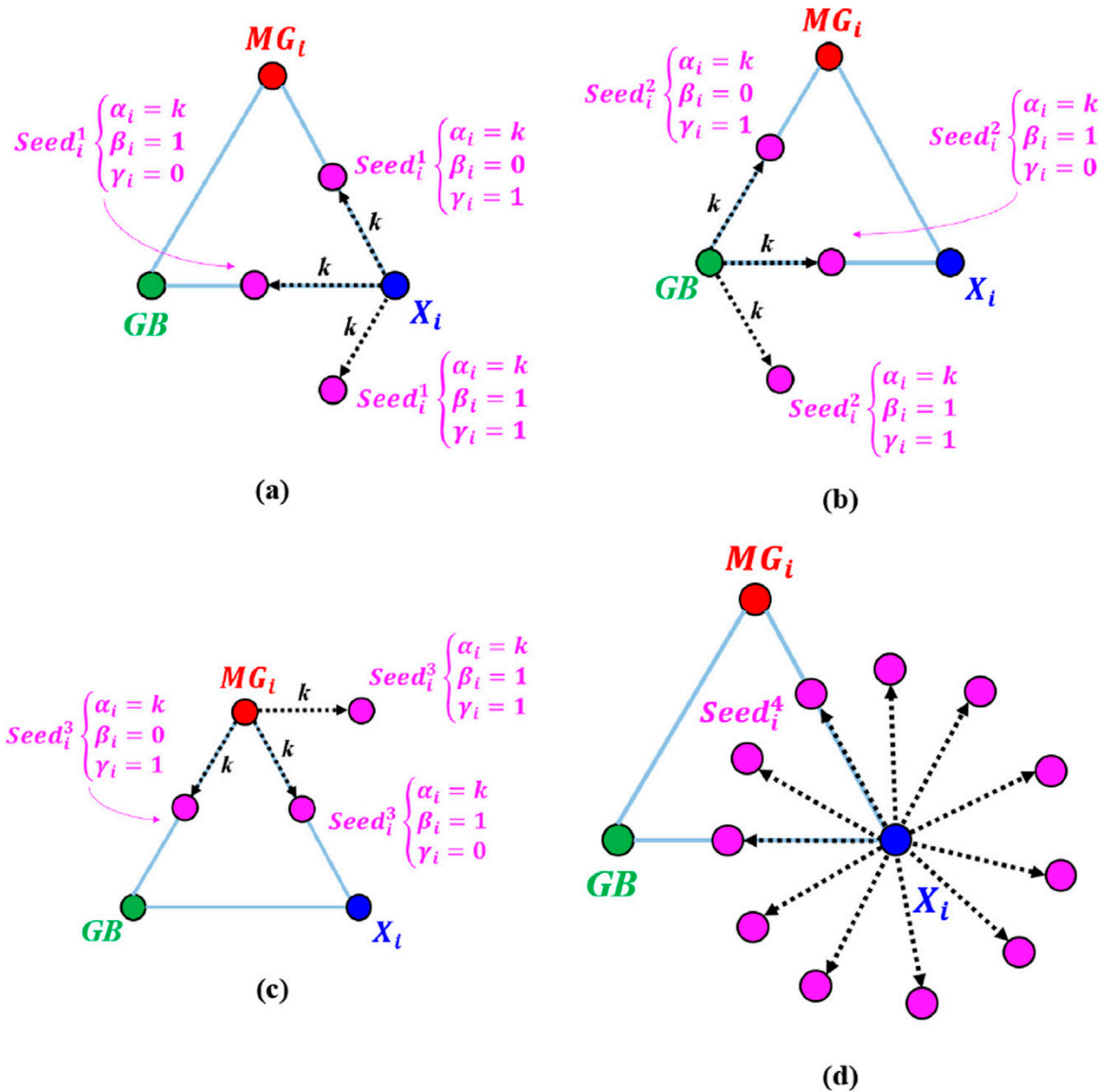


Figure 2. Updating the positions of the temporary triangles [42]. (a) The first seed in the search space; (b) The second seed in the search space; (c) The third seed in the search space; (d) The fourth seed in the search space.

2.3. Optimization of ANN by Chaos Game Optimization

The optimization of ANNs using CGO for predicting blast-induced ground vibration involves fine-tuning the parameters and structure of the neural network to enhance its performance in predicting blast-induced ground vibration. The optimization process is implemented as follows:

- Step 1. Initialization: The optimization process begins by initializing the weights and biases of the ANN model. This involves setting up the initial positions X_i of the solution candidates within the predefined search space, which is often represented as a Sierpiński triangle.
- Step 2. Search loop: The main search loop of the CGO algorithm is executed to adjust the positions of the solution candidates iteratively. Each candidate solution corresponds to a specific set of weights and biases of the ANN model.
- Step 3. Objective function: The performance of each candidate solution (weights and biases) is evaluated using an objective function, which measures how well the ANN model performs in regards to the given task or problem. In this study, RMSE was used as the objective function for the optimization process.
- Step 4. Position updating: During each iteration of the search loop, the positions of the weights and biases are updated based on the CGO algorithm. This involves moving the candidates towards better regions of the search space to improve the performance of the ANN model.
- Step 5. Exploration and exploitation: The movement limitation factor, α_i , is used to balance between exploration (searching for new regions of the search space) and exploitation (exploiting known promising regions). This factor helps control the exploration–exploitation trade-off during the optimization process.
- Step 6. Convergence: The optimization process continues until a stopping criterion is met, such as a maximum number of iterations or achieving a satisfactory level of performance. At this point, the best weights and biases found during the optimization process are selected as the final solution.
- Step 7. Performance evaluation: Finally, the performance of the optimized ANN is evaluated on a separate validation dataset to ensure that it generalizes well to unseen data and performs effectively in real-world scenarios.

The framework of the CGO-ANN model for predicting blast-induced ground vibration is introduced in Figure 3.

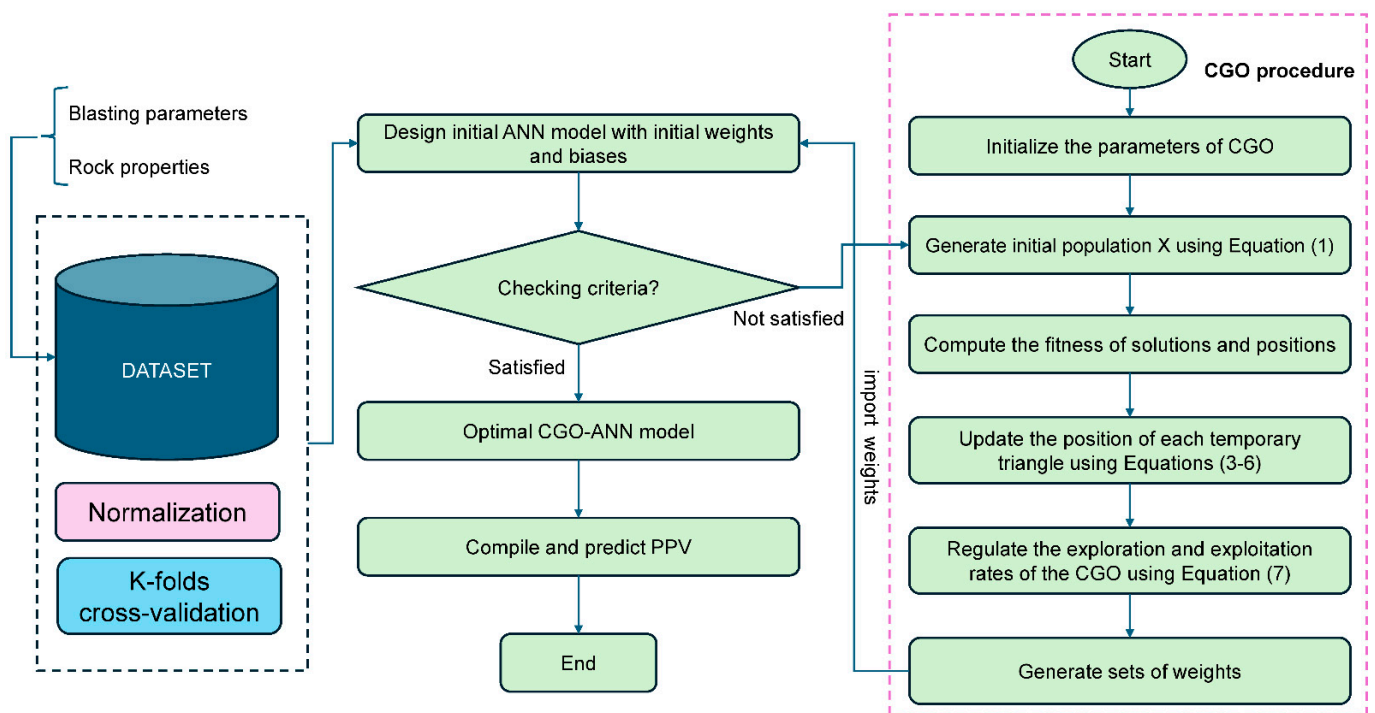


Figure 3. Framework of the CGO-ANN model for predicting blast-induced ground vibration.

3. Application and Experiment Test

3.1. Dataset

To evaluate the efficacy of the proposed CGO-ANN model in predicting PPV induced by mine blasting, we conducted a case study at the Tonglushan Copper Mine in China, as depicted in Figure 4. The geological structure of the area is primarily characterized by the skarn deposit, comprising copper–iron ore, skarn, granodiorite, marble, and other constituents [46,47]. Given the robustness of the rock mass, blasting has been adopted as the principal and efficient method for rock and ore fragmentation in this mine. However, as highlighted in the introduction, its associated adverse effects, particularly ground vibration, are well recognized.

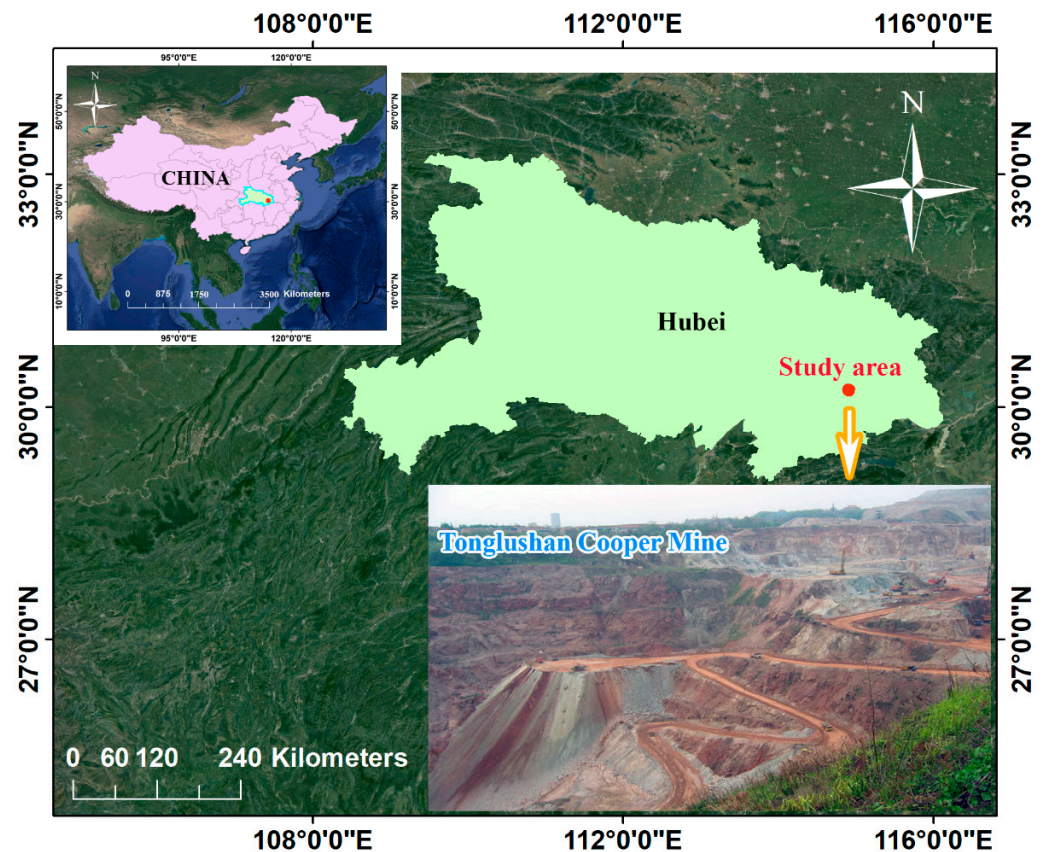
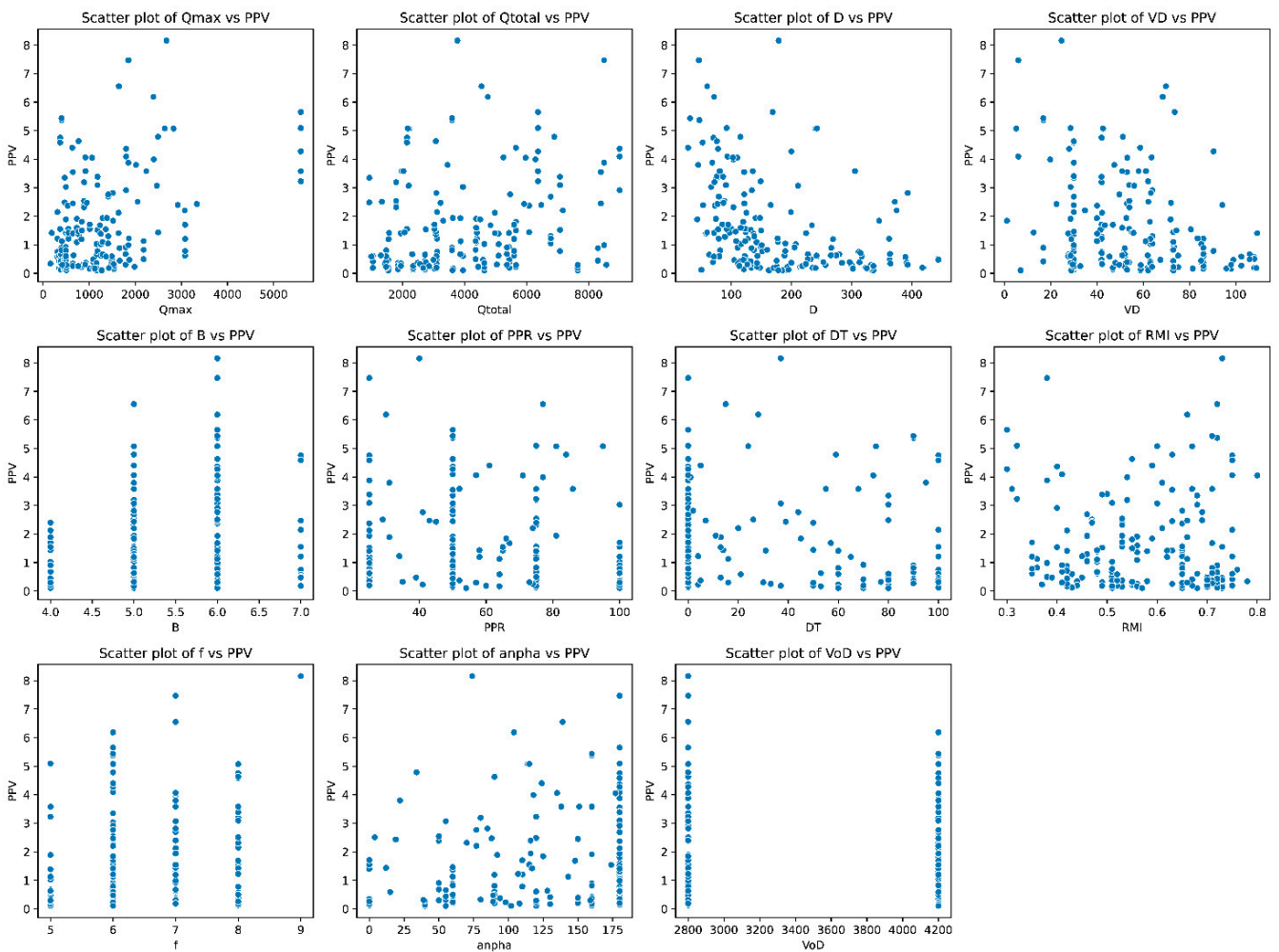


Figure 4. Tonglushan Copper Mine in China.

For the development of PPV predictive models, we gathered and updated data from 180 blasting events conducted at the Tonglushan Copper Mine. Our study considered blasting parameters and rock properties as influential factors affecting PPV, consistent with recommendations from previous researchers [38,47–57]. We collected 11 input variables for PPV prediction, including maximum explosive charged per delay (Q_{\max}), total explosive charged per blast (Q_{total}), monitoring horizontal distance (D), vertical distance (VD), burden (B), pre-crack penetration rate (PPR), delay time (DT), rock mass integrity coefficient (RMI), Protodiakonov's hardness (f), angle between the least resistance line direction and monitoring points (α), and velocity of detonation (VoD). PPVs were recorded by seismographs within a range of 0.101 cm/s to 8.15 cm/s. GPS devices were utilized to ascertain the positions of seismographs and blast sites. Subsequently, horizontal and vertical distances, along with α , were computed based on the GPS results. Rock properties such as PPR, RMI, and f were determined in the laboratory, while the remaining parameters were extracted from the blast patterns. Table 1 provides a summary of some statistical criteria of the dataset, and Figure 5 illustrates visualizations of the dataset.

Table 1. Summary of the blast-induced ground vibration dataset at the Tonglushan Copper Mine.

Q_{max}		Q_{total}		D		VD		B		PPR	
Min.:	160	Min.:	936	Min.:	28.40	Min.:	1.1	Min.:	4.000	Min.:	25.0
1st Qu.:	494	1st Qu.:	2552	1st Qu.:	96.03	1st Qu.:	32.1	1st Qu.:	5.000	1st Qu.:	41.0
Median:	1076	Median:	3952	Median:	141.40	Median:	53.0	Median:	5.000	Median:	50.0
Mean:	1268	Mean:	4195	Mean:	174.18	Mean:	54.8	Mean:	5.389	Mean:	58.2
3rd Qu.:	1636	3rd Qu.:	5600	3rd Qu.:	234.38	3rd Qu.:	73.0	3rd Qu.:	6.000	3rd Qu.:	75.0
Max.:	5590	Max.:	9000	Max.:	444.30	Max.:	109.3	Max.:	7.000	Max.:	100.0
DT		RMI		f		α		VoD		PPV	
Min.:	0.00	Min.:	0.3000	Min.:	5.000	Min.:	0.00	Min.:	2800	Min.:	0.1010
1st Qu.:	0.00	1st Qu.:	0.4700	1st Qu.:	6.000	1st Qu.:	76.25	1st Qu.:	2800	1st Qu.:	0.3862
Median:	1.50	Median:	0.5550	Median:	6.000	Median:	130.00	Median:	2800	Median:	1.0380
Mean:	30.96	Mean:	0.5656	Mean:	6.489	Mean:	121.03	Mean:	3430	Mean:	1.6262
3rd Qu.:	68.50	3rd Qu.:	0.6725	3rd Qu.:	7.000	3rd Qu.:	180.00	3rd Qu.:	4200	3rd Qu.:	2.4065
Max.:	100.00	Max.:	0.8000	Max.:	9.000	Max.:	180.00	Max.:	4200	Max.:	8.1580



(a)

Figure 5. Cont.

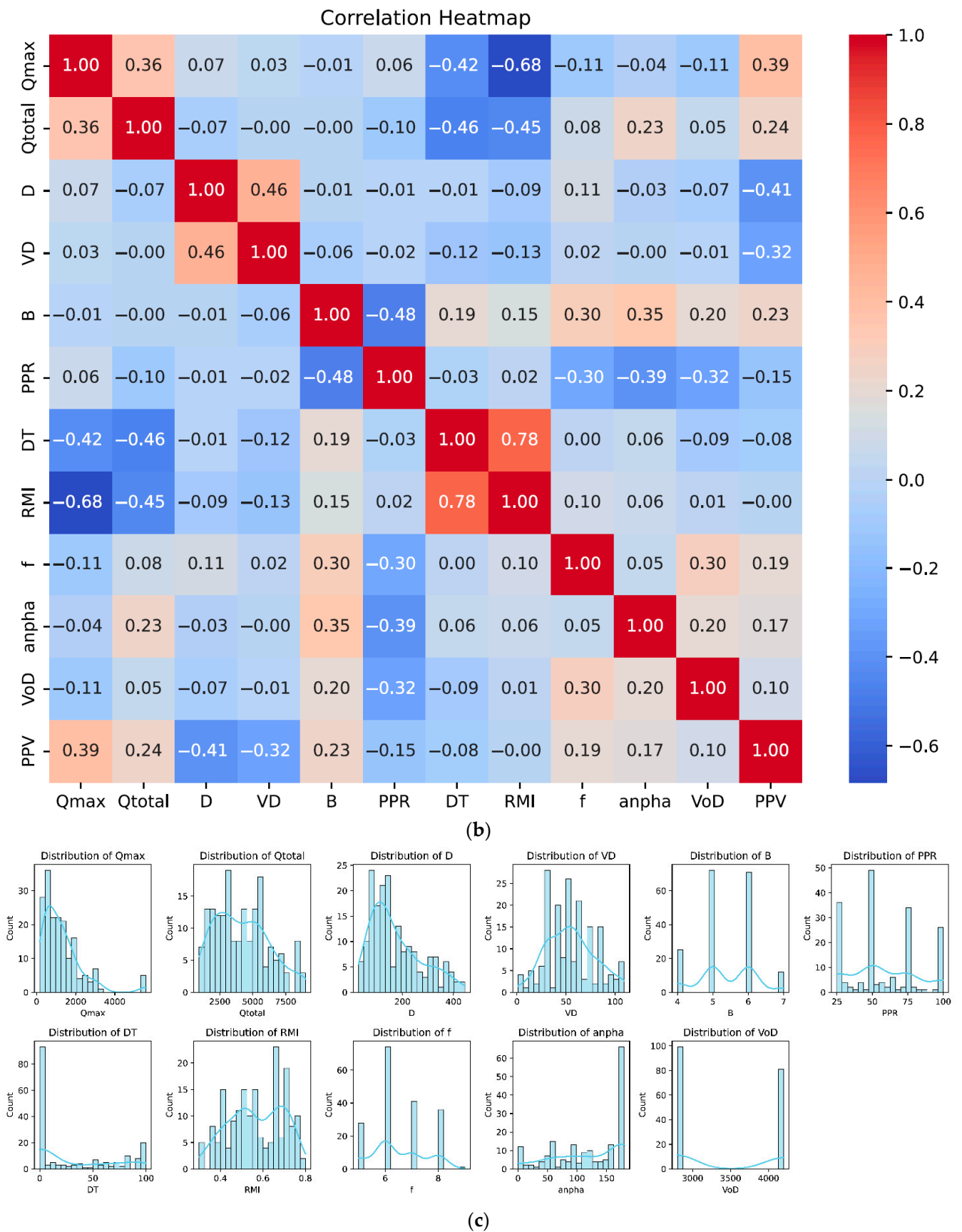


Figure 5. Visualization of the blast-induced ground vibration dataset at the Tonglushan Copper Mine. (a) Scatter plot of each independent variable; (b) correlation heatmap; (c) distribution plots of variables.

The dataset comprising 180 blasts at the Tonglushan Copper Mine in China indeed offers valuable insights into the blasting practices and outcomes specific to this mine. Figure 5 illustrates the extensive range of data, particularly concerning parameters like explosive charge per delay (Q_{\max}), Q_{total} , D , VD , DT , RMI , and α .

Referring to Table 1, which summarizes the blast-induced ground vibration dataset at the Tonglushan Copper Mine, we can observe a diverse distribution of key metrics such as Q_{\max} , Q_{total} , D , VD , B , PPR , DT , RMI , f , α , VoD , and PPV . These metrics provide a comprehensive overview of the blasting activities and their resulting ground vibrations, encompassing various aspects of the blasting process and its effects.

Considering the breadth and depth of this dataset, it is reasonable to assert that the information generated from these 180 blasts is likely to be representative of the blasting practices and outcomes at the Tonglushan Copper Mine. This dataset can serve as a valuable resource for analyzing and optimizing blasting operations, as well as for developing models and strategies to minimize environmental impacts and enhance safety.

3.2. Model Development

Before predictive models for blast-induced ground vibration prediction were developed, the dataset underwent normalization to prevent data leakage, in which information from validation or test sets inadvertently influences the training process. In this study, the min-max normalization technique was utilized to scale the features (consisting of 11 variables from the blast-induced ground vibration dataset) to a similar range, aiding in the facilitation of learning.

For the development of the CGO-ANN model predicting PPV , the collected dataset comprising 180 samples was partitioned into two parts. A total of 70% of the dataset was randomly selected as the training dataset to optimize the weights and biases of the ANN model. Meanwhile, the remaining 30% was reserved for testing the model's performance.

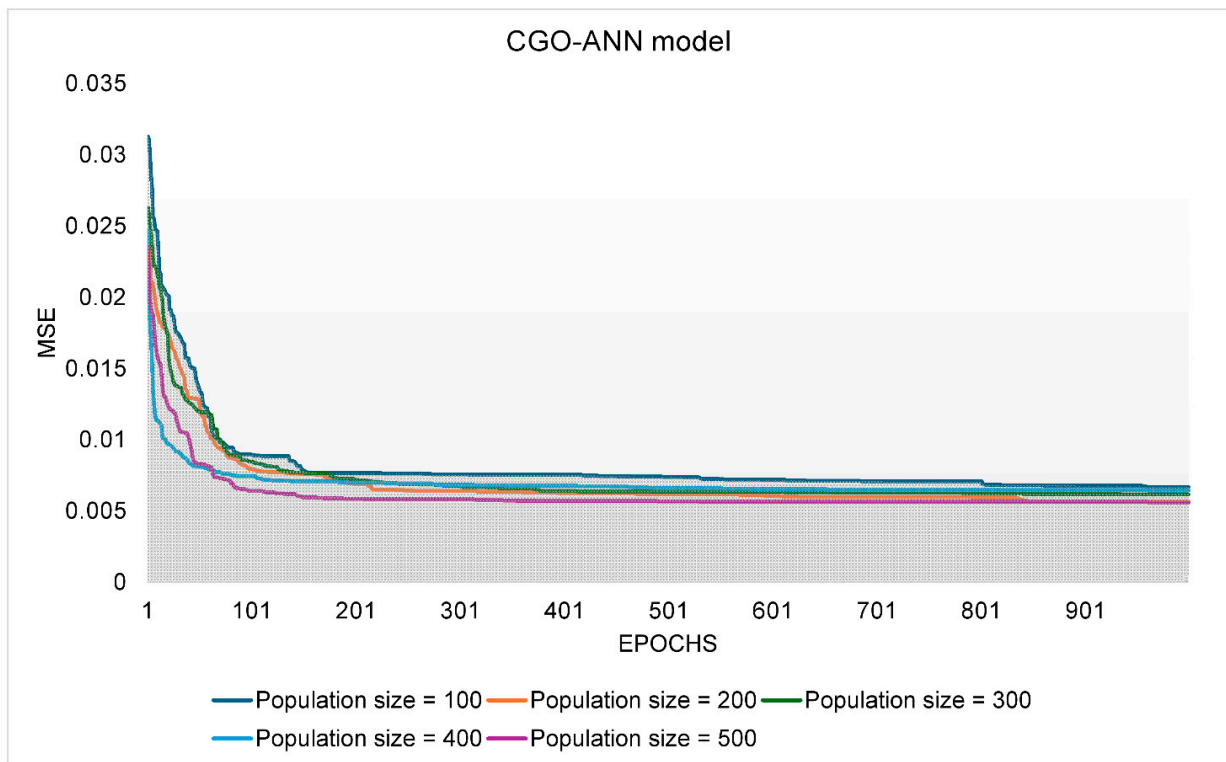
It is important to highlight that this study not only proposes and develops the CGO-ANN model but also introduces the PSO-ANN, GA-ANN, single ANN, and USBM empirical models for comparison purposes, evaluating the superiority of the proposed CGO-ANN model. For the hybrid models like CGO-ANN, GA-ANN, and PSO-ANN, the initial parameters of the metaheuristic algorithms play a crucial role in enhancing the optimization processes for predicting PPV . These initial parameters are configured as follows:

- GA: crossover coefficient = 0.85; mutation coefficient = 0.05.
- PSO: local coefficient = global coefficient = 1.2; weight min coefficient = 0.4; weight max coefficient = 0.9.
- CGO: using the number of populations and iterations.

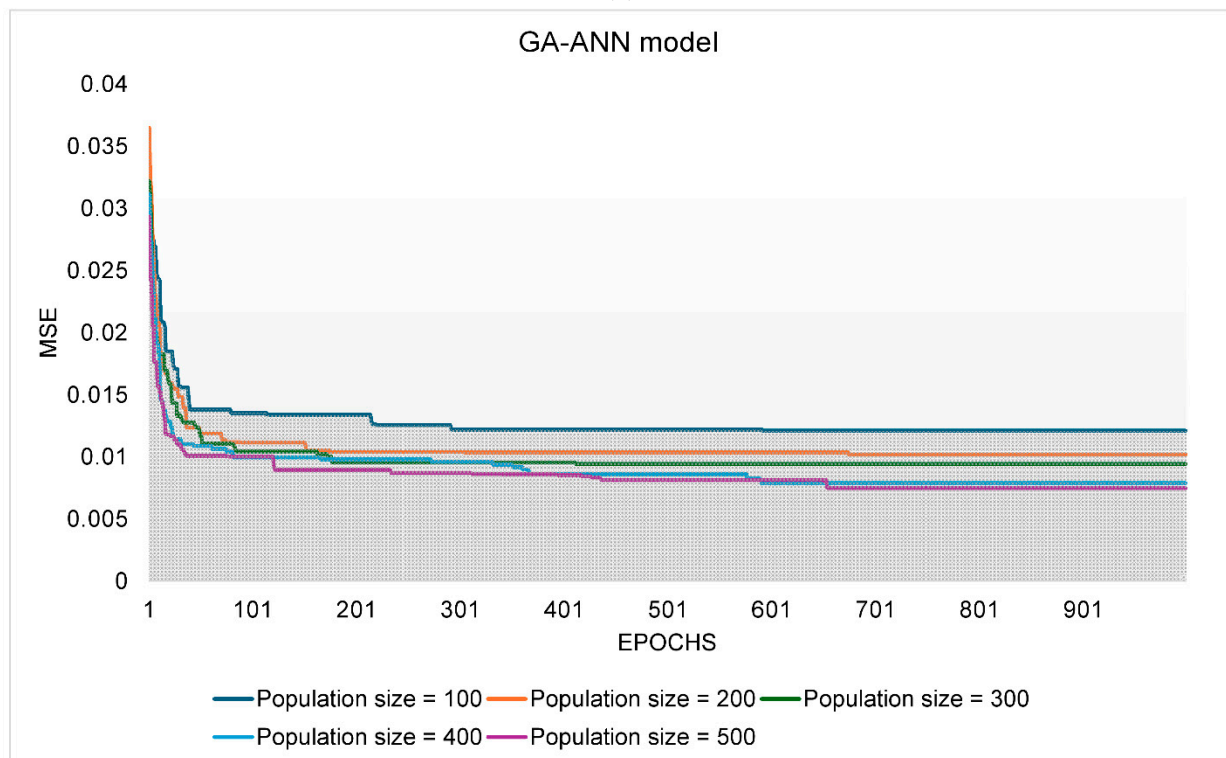
Furthermore, all these algorithms are implemented with varying initial population diversities (i.e., 100, 200, 300, 400, 500), and the optimization process spans 1000 iterations.

An initial ANN structure with a single hidden layer containing 15 hidden neurons was chosen for this study, utilizing the ReLU activation function. MSE (mean-squared error) served as the objective function for these hybrid models during the training process. The development and optimization process of the CGO-ANN, PSO-ANN, and GA-ANN models are illustrated in Figure 6.

Furthermore, alongside the hybrid models, a standalone ANN was developed for predicting PPV and contrasting it with the proposed CGO-ANN model. The identical datasets, encompassing both training and testing datasets, normalization technique, and structure, were employed in constructing the standalone ANN model. However, in this instance, the backpropagation algorithm was employed to train the ANN model, representing the most prevalent algorithm traditionally used for ANN model training. The performance of the ANN model development is depicted in Figure 7.

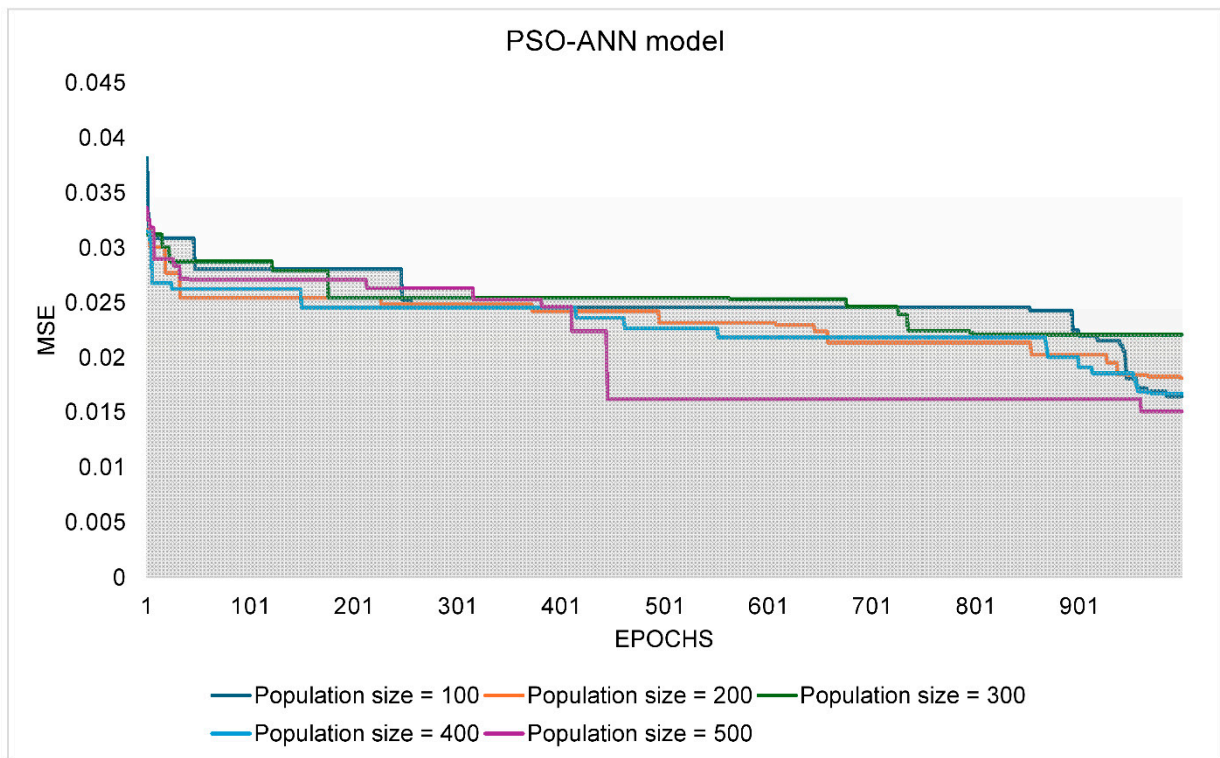


(a)



(b)

Figure 6. Cont.



(c)

Figure 6. Optimization process of the hybrid models for PPV prediction under different population sizes. (a) CGO-ANN model; (b) GA-ANN model; (c) PSO-ANN model.

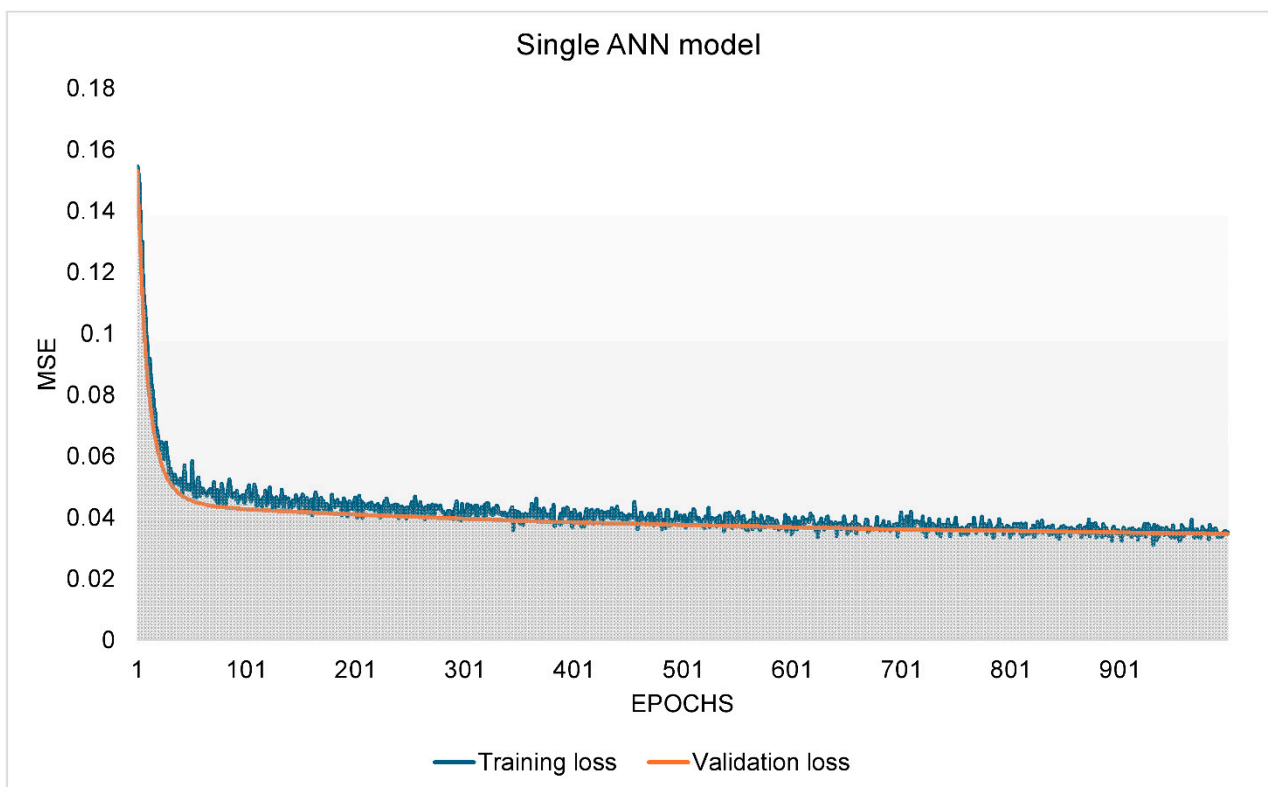


Figure 7. Development process of the single ANN model for PPV prediction.

The USBM (United States Bureau of Mines) empirical equation stands as one of the most frequently utilized equations for swiftly gauging the intensity of PPV in blasting. This equation was pioneered by Duvall and Fogelson [58] and relies on historical data and regression analysis for its computation. It is worth mentioning that the identical datasets will be employed in establishing the USBM empirical equation, which is ultimately formulated to estimate PPV in the following manner:

$$PPV = 1.684 \left(\frac{D}{\sqrt{Q_{\max}}} \right)^{-0.337} \quad (8)$$

According to the USBM equation, the horizontal distance (D) and maximum explosive charge per delay (Q_{\max}) should be used to calculate PPV.

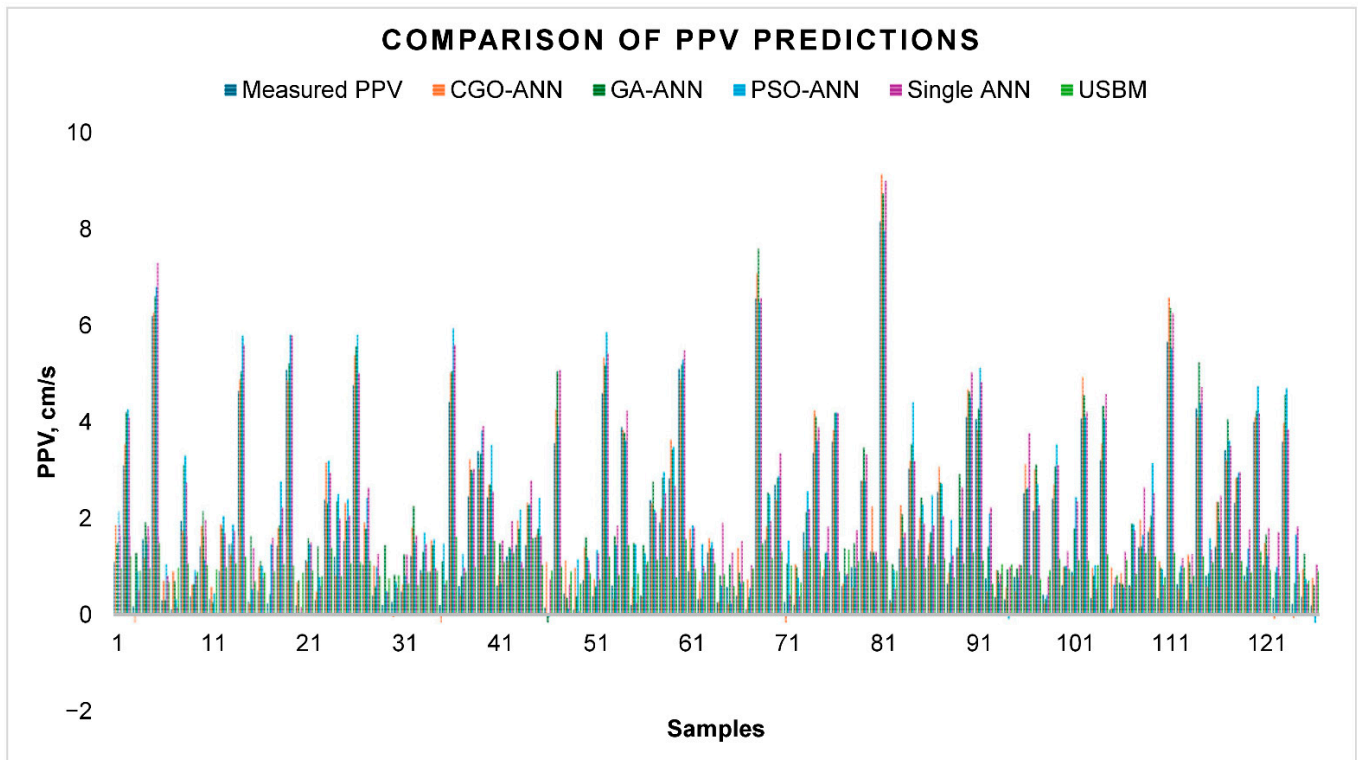
4. Results and Discussion

In this section, we present the results and discuss the findings of our study aimed at predicting blast-induced ground vibration. Our study focused on developing and evaluating predictive models to estimate PPV, which is a crucial parameter for assessing the potential impact of blasting operations on nearby structures and the surrounding environment. We specifically investigated the performance of the CGO-ANN, GA-ANN, PSO-ANN, single ANN, and USBM models, with a particular emphasis on the proposed novel CGO-ANN model. The outcome predictions of the CGO-ANN, GA-ANN, PSO-ANN, single ANN, and USBM models are shown in Figure 8 for both training and testing datasets.

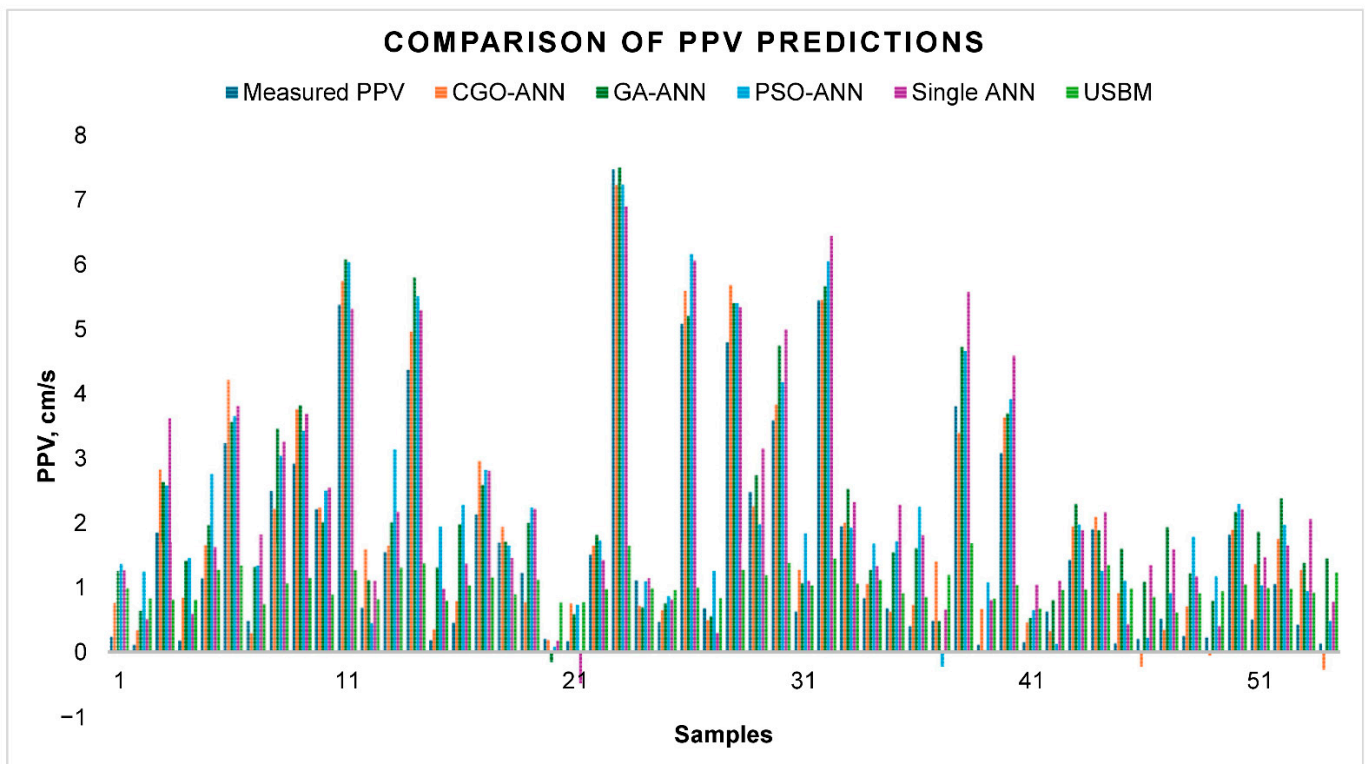
The outcomes depicted in Figure 8 showcased diverse performance levels among various algorithms, with certain models demonstrating superior accuracy and predictive capability over others. Notably, the CGO-ANN model, introduced as a novel approach in this study, exhibited particularly promising results, surpassing other models in terms of accuracy and predictive capacity. Conversely, the USBM model displayed the weakest performance in predicting PPV across both training and testing datasets.

Figure 9 illustrates a scatter plot correlating the measured PPVs with the predicted PPVs to assess the accuracy of each model in predicting blast-induced ground vibration. The findings revealed that the CGO-ANN and GA-ANN models offered greater accuracy in PPV prediction compared to the other models. Furthermore, the hybrid models, including CGO-ANN, GA-ANN, and PSO-ANN, demonstrated enhancements over the single ANN model in predicting PPV within the Tonglushan Copper Mine of China. Conversely, the empirical model (USBM) exhibited the highest errors in regards to PPV estimation.

To delve deeper into the predictive capabilities of each model in forecasting PPV, in our study, we undertook a regression analysis using both measured and predicted PPV values, as depicted in Figure 10. Our analyses revealed that the hybrid ANN models exhibited superior convergence compared to the single ANN model, with particular emphasis on the CGO-ANN model. Notably, the predicted data points from the CGO-ANN model clustered closer to the regression line than did those from the other models. Additionally, as depicted in Figure 10, the confidence level of the developed models is illustrated with a 95% confidence interval (highlighted by the grey areas). Notably, the majority of the predicted datasets from the CGO-ANN model fall within this interval, surpassing the performance of the GA-ANN model and other models showcased in the figure. It is significant that the USBM empirical model displayed the least accuracy and convergence, indicating a notable disparity between its predicted and actual values. To precisely assess the performance of the developed models, we computed various performance metrics, including mean squared error (MSE), root mean squared error (RMSE), mean absolute error (MAE), and determination coefficient (R^2) based on both the measured and predicted PPV values. These metrics are presented in Table 2 for comprehensive evaluation.



(a)



(b)

Figure 8. The outcome predictions of PPV under the models developed: (a) training samples; (b) testing samples.

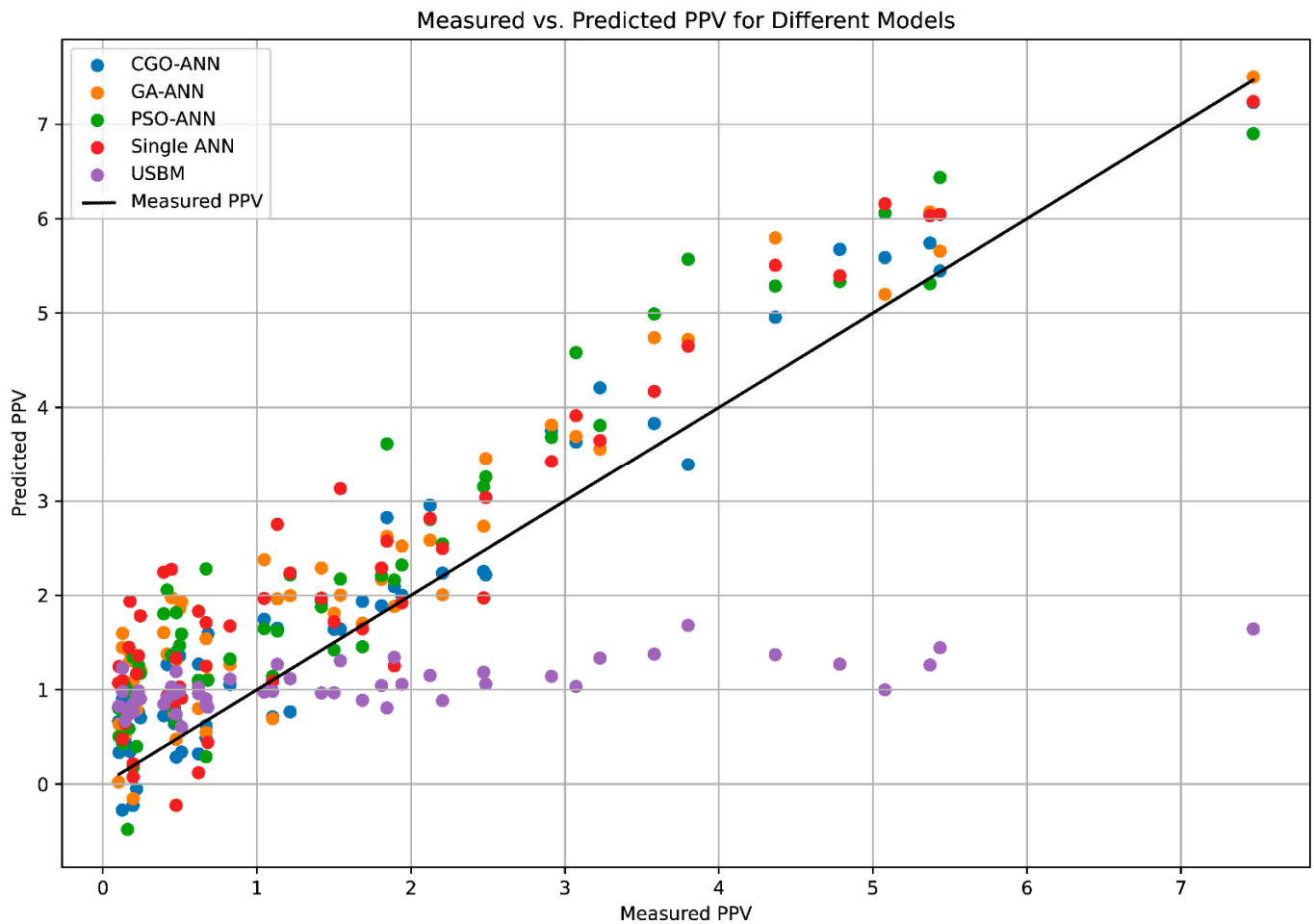


Figure 9. Scatter plot of the measured vs. predicted PPV for different models.

Table 2. Performance indicators of the developed models.

PPV Predictive Model	Training Dataset				Testing Dataset			
	MSE	RMSE	MAE	R ²	MSE	RMSE	MAE	R ²
CGO-ANN	0.261	0.511	0.426	0.899	0.259	0.508	0.425	0.909
GA-ANN	0.436	0.660	0.555	0.832	0.637	0.798	0.669	0.777
PSO-ANN	0.547	0.740	0.620	0.789	0.720	0.848	0.719	0.748
Single ANN	0.566	0.752	0.624	0.782	0.770	0.877	0.745	0.731
USBM	2.589	1.609	1.053	0.384	2.672	1.635	1.102	0.520

The performance evaluation of the PPV predictive models provides compelling evidence supporting the superiority of the CGO-ANN model. Across both the training and testing datasets, the CGO-ANN model consistently yields lower MSE, RMSE, and MAE values compared to the other models. For instance, in the testing dataset, the CGO-ANN model exhibits an MSE of 0.259, whereas the GA-ANN, PSO-ANN, single ANN, and USBM models record MSE values of 0.637, 0.720, 0.770, and 2.672, respectively. Similarly, the CGO-ANN model achieves an RMSE of 0.508 and an MAE of 0.425 in the testing dataset, outperforming all other models.

Moreover, the R² values further reinforce the superiority of the CGO-ANN model in explaining the variance in PPV. The CGO-ANN model demonstrates substantially higher R² values compared to the other models, indicating its superior ability to capture the underlying relationships between input variables and PPV. For instance, in the testing dataset, the CGO-ANN model achieves an R² value of 0.909, while the GA-ANN, PSO-

ANN, single ANN, and USBM models record R^2 values of 0.777, 0.748, 0.731, and 0.520, respectively. Based on the results depicted in Figure 10, the reliability range of the proposed CGO-ANN model, determined by the significance level of the estimates, falls within the range of 89% to 91%. In contrast, other models exhibited reliability ranges between 50% and 80%.

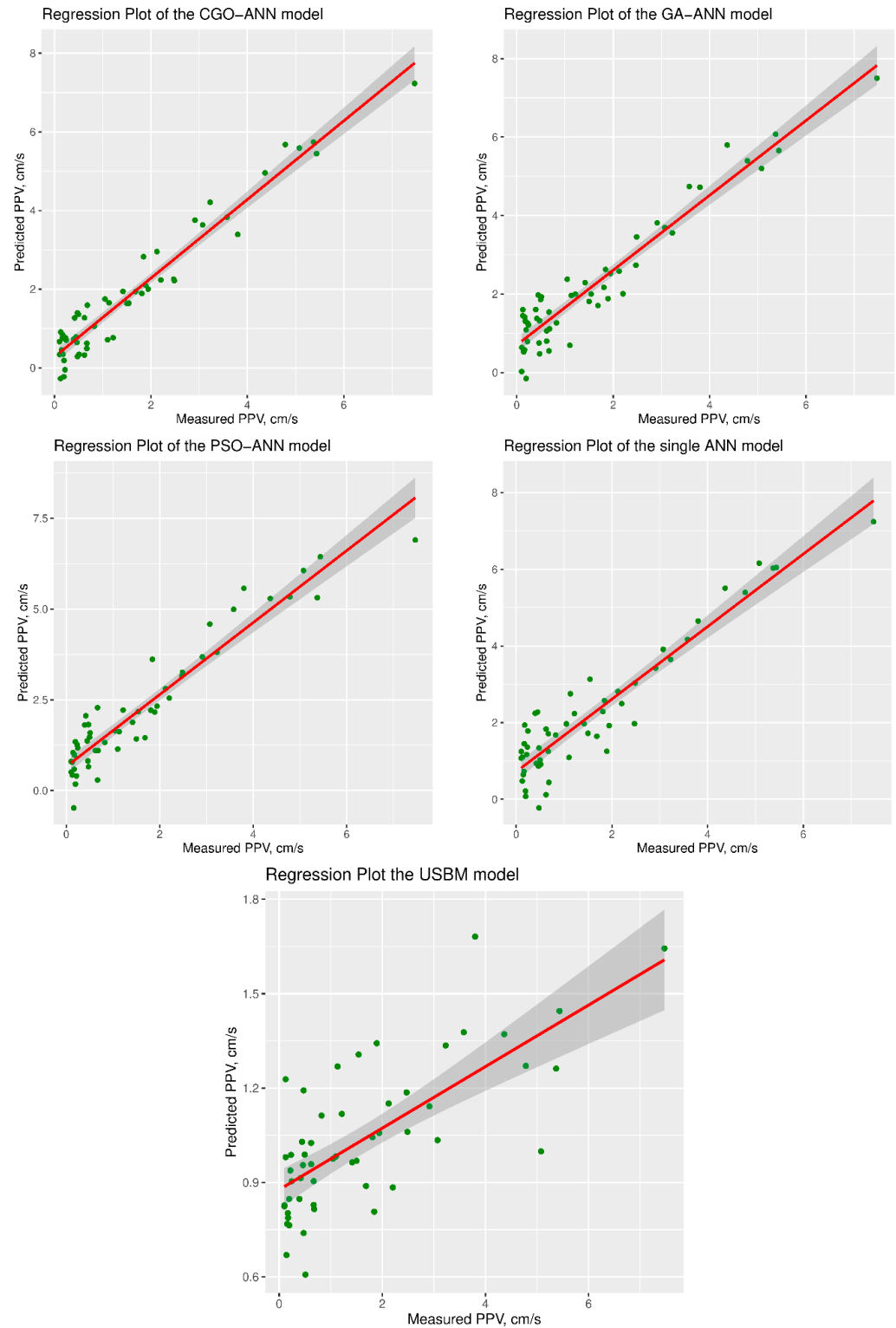


Figure 10. Regression analysis of the outcome predictions on the testing dataset, with a 95% confidence interval.

These numerical results provided strong evidence supporting the efficacy of the CGO-ANN model in accurately predicting PPV. The consistently lower prediction errors and higher R^2 values demonstrated the superior performance of the CGO-ANN model compared to traditional ANN models and the empirical USBM model. Therefore, based on the numerical evidence, it can be concluded that the CGO-ANN model is the most effective predictive model for PPV estimation in this study. In Figure 11, we evaluate the developed models through the distribution of residuals.

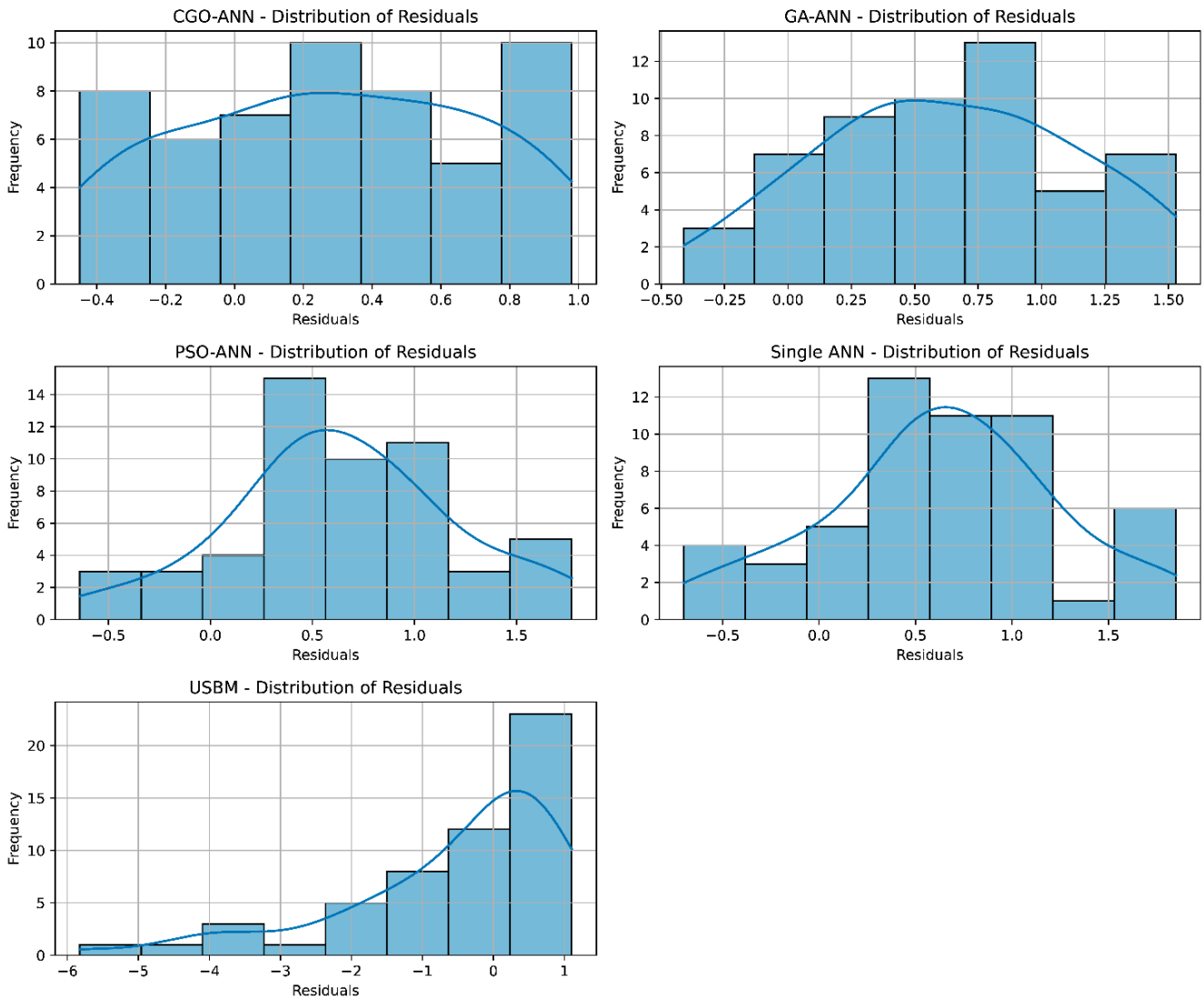


Figure 11. Distribution of residuals for each PPV predictive model developed.

The distribution of residuals provides crucial insights into the accuracy and reliability of the predictive models. Ideally, the residuals should follow a normal distribution, indicating that the model effectively captures the underlying patterns in the data. A normal distribution of residuals suggests that the model accurately accounts for the variability in PPV, with the errors evenly distributed around zero. This implies that the model predicts PPV values with minimal bias and consistent accuracy across the range of observed PPV values. From Figure 11, we can see that the CGO-ANN model follows a normal distribution, indicating that this model effectively captures the underlying patterns in the data. Meanwhile, the other models, such as GA-ANN, PSO-ANN, single ANN, and the USBM model, yielded deviations from a normal distribution of residuals, and this could indicate potential issues with the predictive models, such as the model systematically underestimating or overestimating PPV values in certain ranges. In the GA-ANN, PSO-ANN, single ANN, and

USBM models, all of their residuals are positively skewed, indicating that the models tend to underestimate PPV in higher ranges, whereas negatively skewed residuals suggest underestimation in lower ranges. In addition, heteroscedastic residuals imply that the spread of errors varies across different levels of PPV. This suggests that the model's predictions are less reliable for certain ranges of PPV values, leading to inconsistent prediction accuracy.

To directly assess the normality of the residuals, a Q–Q plot was employed, providing a clearer indication of deviations from the expected normal distribution. By comparing the observed quantiles of residuals to those of a theoretical normal distribution, as demonstrated in Figure 12, we obtain a more nuanced understanding of residual normality for each PPV predictive model. This integrated approach strengthens the evaluation process, ensuring a thorough examination and resolution of any deviations from normality. Notably, the analysis of Figure 12 highlights insights provided by the CGO-ANN and GA-ANN models regarding specific deviations, aiding in pinpointing areas for model improvement. Specifically, these models exhibit deviations when the residuals of PPV predictions exceed 2 cm/s or fall below -2 cm/s. Conversely, the single ANN model and the USBM model demonstrate pronounced skewness in the residuals, indicating heavy tails or other deviations from normality. These findings underscore the need for further enhancements to these models to ensure more accurate and reliable PPV estimation.

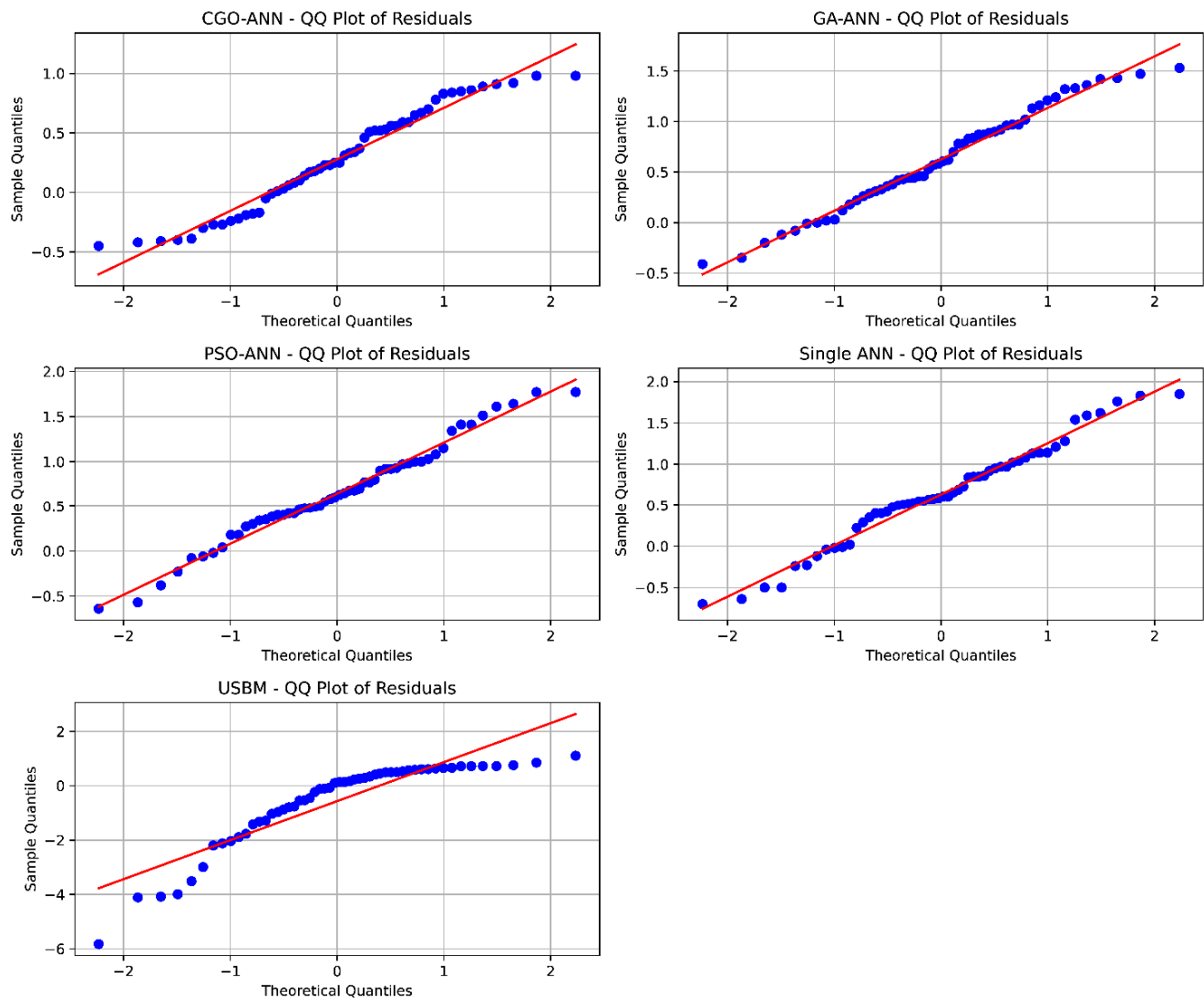


Figure 12. Q–Q plot of residuals for each PPV predictive model developed.

From the findings and analyses of this study, it is evident that the proposed CGO-ANN model emerges as a novel and robust approach for predicting PPV, demonstrating superior performance and reliability. Compared to alternative optimized models such as GA-ANN and PSO-ANN, the CGO-ANN model exhibits notable proficiency in PPV prediction, indicating the compatibility of chaos theory with the inherent uncertainties of PPV propagation in the ground. Furthermore, this study underscores the unsuitability of the USBM model for PPV prediction due to its low reliability.

5. Conclusions

In this study, we explored various predictive models for estimating PPV in blast-induced ground vibration scenarios. By leveraging machine learning techniques and empirical modeling, we aimed to develop robust models capable of accurately predicting PPV, a critical parameter for assessing the potential impacts of blasting operations on surrounding structures and the environment.

Our analysis revealed compelling insights into the performance of different predictive models. Among the models evaluated, the proposed CGO-ANN model emerged as a stand-out, demonstrating superior predictive accuracy and reliability compared to alternative optimized models, including GA-ANN and PSO-ANN. The CGO-ANN model, rooted in chaos theory, proved particularly adept at capturing the uncertainties inherent in PPV propagation through the ground, showcasing its potential as a novel approach for PPV prediction.

Furthermore, our study highlighted the limitations of traditional empirical models, such as the USBM model, in accurately predicting PPV. Despite its widespread use, the USBM model exhibited low reliability in our analysis, reaffirming the need for more advanced modeling techniques to address the complexities of blast-induced ground vibration.

Finally, our study contributes to the advancement of blast management practices and environmental stewardship by offering improved methodologies for assessing and mitigating the impacts of blasting operations. Moving forward, further research efforts should focus on refining and validating predictive models, incorporating additional factors influencing PPV, and conducting field validation studies to enhance the applicability and robustness of PPV prediction models in real-world scenarios.

Although the obtained results are promising, there are several limitations to consider. The study primarily focuses on PPV prediction in blast-induced ground vibration scenarios, potentially limiting its applicability to other types of vibration prediction or mining-related parameters. Additionally, the dataset used for model development and evaluation is derived from a single mining site, which may not fully represent the diversity of blasting conditions and geological settings encountered in other mining operations. Furthermore, the analysis may overlook certain factors influencing PPV that were not included in the dataset, such as variations in geological structures, weather conditions, or blasting techniques.

In light of these limitations, future research directions should include investigating the applicability of the CGO-ANN model and other predictive models in different mining sites and geological contexts to assess their generalizability. Exploring the incorporation of additional variables or features into the predictive models to enhance their accuracy and robustness, considering factors like geological properties, weather conditions, and blast design parameters, is also warranted. Additionally, conducting field validation studies to validate the performance of predictive models in real-world blasting scenarios and assess their practical utility and reliability will be beneficial.

Author Contributions: Conceptualization, S.Z. and M.C.; Methodology, S.Z., L.W. and M.C.; Formal analysis, L.W.; Investigation, M.C.; Data curation, S.Z.; Writing—original draft, S.Z., L.W. and M.C.; Writing—review & editing, S.Z., L.W. and M.C.; Visualization, L.W. All authors have read and agreed to the published version of the manuscript.

Funding: This research was supported by the National Key R&D Program of China (Grant No. 2022YFC2904105).

Institutional Review Board Statement: Not applicable.

Informed Consent Statement: Not applicable.

Data Availability Statement: The original contributions presented in the study are included in the article, further inquiries can be directed to the corresponding author.

Conflicts of Interest: The authors declare no conflict of interest.

References

1. Elevli, B.; Arpaz, E. Evaluation of parameters affected on the blast induced ground vibration (BIGV) by using relation diagram method (RDM). *Acta Montan. Slovaca* **2010**, *15*, 261.
2. Khandelwal, M. Evaluation and prediction of blast-induced ground vibration using support vector machine. *Int. J. Rock Mech. Min. Sci.* **2010**, *47*, 509–516. [[CrossRef](#)]
3. Hagan, T. Rock breakage by explosives. In *Gasdynamics of Explosions and Reactive Systems*; Elsevier: Amsterdam, The Netherlands, 1980; pp. 329–340.
4. Xue, X.; Yang, X. Predicting blast-induced ground vibration using general regression neural network. *J. Vib. Control* **2014**, *20*, 1512–1519. [[CrossRef](#)]
5. Görgülü, K.; Arpaz, E.; Demirci, A.; Koçaslan, A.; Dilmaç, M.K.; Yüksek, A.G. Investigation of blast-induced ground vibrations in the Tülü boron open pit mine. *Bull. Eng. Geol. Environ.* **2013**, *72*, 555–564. [[CrossRef](#)]
6. Qiu, Y.; Zhou, J. Short-term rockburst damage assessment in burst-prone mines: An explainable XGBOOST hybrid model with SCSO algorithm. *Rock Mech. Rock Eng.* **2023**, *56*, 8745–8770. [[CrossRef](#)]
7. Zhou, J.; Zhang, Y.; Qiu, Y. State-of-the-art review of machine learning and optimization algorithms applications in environmental effects of blasting. *Artif. Intell. Rev.* **2024**, *57*, 5. [[CrossRef](#)]
8. Qiu, Y.; Zhou, J. Short-term rockburst prediction in underground project: Insights from an explainable and interpretable ensemble learning model. *Acta Geotech.* **2023**, *18*, 6655–6685. [[CrossRef](#)]
9. Nateghi, R. Evaluation of blast induced ground vibration for minimizing negative effects on surrounding structures. *Soil Dyn. Earthq. Eng.* **2012**, *43*, 133–138. [[CrossRef](#)]
10. Yan, Y.; Hou, X.; Fei, H. Review of predicting the blast-induced ground vibrations to reduce impacts on ambient urban communities. *J. Clean. Prod.* **2020**, *260*, 121135. [[CrossRef](#)]
11. Shin, J.-H.; Moon, H.-G.; Chae, S.-E. Effect of blast-induced vibration on existing tunnels in soft rocks. *Tunn. Undergr. Space Technol.* **2011**, *26*, 51–61. [[CrossRef](#)]
12. Thoenen, J.R.; Thoenen, J.R.; Windes, S. *Seismic Effects of Quarry Blasting*; United States Department of the Interior, Bureau of Mines: Washington, DC, USA, 1942.
13. Langefors, U.; Kihlström, B. *The Modern Technique of Rock Blasting*; John & Wiley & Sons: Hoboken, NJ, USA, 1963.
14. Ambraseys, N.N.; Hendron, A. *Dynamic Behaviour of Rock Masses*; John & Wiley & Sons: Hoboken, NJ, USA, 1968.
15. Roy, P.P. Putting ground vibration predictions into practice. *Colliery Guard.* **1993**, *241*, 63–67, 70.
16. Rai, R.; Shrivastva, B.; Singh, T. Prediction of maximum safe charge per delay in surface mining. *Min. Technol.* **2005**, *114*, 227–231. [[CrossRef](#)]
17. Matidza, M.I.; Jianhua, Z.; Gang, H.; Mwangi, A.D. Assessment of blast-induced ground vibration at Jinduicheng molybdenum open pit mine. *Nat. Resour. Res.* **2020**, *29*, 831–841. [[CrossRef](#)]
18. Dumakor-Dupey, N.K.; Arya, S.; Jha, A. Advances in blast-induced impact prediction—A review of machine learning applications. *Minerals* **2021**, *11*, 601. [[CrossRef](#)]
19. Zhang, H.; Zhou, J.; Jahed Armaghani, D.; Tahir, M.; Pham, B.T.; Huynh, V.V. A combination of feature selection and random forest techniques to solve a problem related to blast-induced ground vibration. *Appl. Sci.* **2020**, *10*, 869. [[CrossRef](#)]
20. Ragam, P.; Nimaje, D.S. Evaluation and prediction of blast-induced peak particle velocity using artificial neural network: A case study. *Noise Vib. Worldw.* **2018**, *49*, 111–119. [[CrossRef](#)]
21. Saeidi, O.; Torabi, S.R.; Ataei, M. Prediction of the rock mass diggability index by using fuzzy clustering-based, ANN and multiple regression methods. *Rock Mech. Rock Eng.* **2014**, *47*, 717–732. [[CrossRef](#)]
22. Azimi, Y.; Khoshrou, S.H.; Osanloo, M. Prediction of blast induced ground vibration (BIGV) of quarry mining using hybrid genetic algorithm optimized artificial neural network. *Measurement* **2019**, *147*, 106874. [[CrossRef](#)]
23. Alipour, A.; Mokhtarian, M.; Abdollahei Sharif, J. Artificial neural network or empirical criteria? A comparative approach in evaluating maximum charge per delay in surface mining—Sungun copper mine. *J. Geol. Soc. India* **2012**, *79*, 652–658. [[CrossRef](#)]
24. Mohamed, M.T. Artificial neural network for prediction and control of blasting vibrations in Assiut (Egypt) limestone quarry. *Int. J. Rock Mech. Min. Sci.* **2009**, *46*, 426–431. [[CrossRef](#)]
25. Khandelwal, M.; Singh, T. Prediction of blast-induced ground vibration using artificial neural network. *Int. J. Rock Mech. Min. Sci.* **2009**, *46*, 1214–1222. [[CrossRef](#)]

26. Zhou, J.; Shen, X.; Qiu, Y.; Shi, X.; Du, K. Microseismic location in hardrock metal mines by machine learning models based on hyperparameter optimization using bayesian optimizer. *Rock Mech. Rock Eng.* **2023**, *56*, 8771–8788. [[CrossRef](#)]
27. Shirani Faradonbeh, R.; Jahed Armaghani, D.; Abd Majid, M.; Md Tahir, M.; Ramesh Murlidhar, B.; Monjezi, M.; Wong, H. Prediction of ground vibration due to quarry blasting based on gene expression programming: A new model for peak particle velocity prediction. *Int. J. Environ. Sci. Technol.* **2016**, *13*, 1453–1464. [[CrossRef](#)]
28. Zhou, J.; Shi, X.; Li, X. Utilizing gradient boosted machine for the prediction of damage to residential structures owing to blasting vibrations of open pit mining. *J. Vib. Control* **2016**, *22*, 3986–3997. [[CrossRef](#)]
29. Armaghani, D.J.; Momeni, E.; Abad, S.V.A.N.K.; Khandelwal, M. Feasibility of ANFIS model for prediction of ground vibrations resulting from quarry blasting. *Environ. Earth Sci.* **2015**, *74*, 2845–2860. [[CrossRef](#)]
30. Faradonbeh, R.S.; Monjezi, M. Prediction and minimization of blast-induced ground vibration using two robust meta-heuristic algorithms. *Eng. Comput.* **2017**, *33*, 835–851. [[CrossRef](#)]
31. Zhang, X.; Nguyen, H.; Bui, X.-N.; Tran, Q.-H.; Nguyen, D.-A.; Bui, D.T.; Moayed, H. Novel soft computing model for predicting blast-induced ground vibration in open-pit mines based on particle swarm optimization and XGBoost. *Nat. Resour. Res.* **2020**, *29*, 711–721. [[CrossRef](#)]
32. Yang, H.; Hasanipanah, M.; Tahir, M.; Bui, D.T. Intelligent prediction of blasting-induced ground vibration using ANFIS optimized by GA and PSO. *Nat. Resour. Res.* **2020**, *29*, 739–750. [[CrossRef](#)]
33. Bui, X.-N.; Choi, Y.; Atrushkevich, V.; Nguyen, H.; Tran, Q.-H.; Long, N.Q.; Hoang, H.-T. Prediction of blast-induced ground vibration intensity in open-pit mines using unmanned aerial vehicle and a novel intelligence system. *Nat. Resour. Res.* **2020**, *29*, 771–790. [[CrossRef](#)]
34. Xue, X. Neuro-fuzzy based approach for prediction of blast-induced ground vibration. *Appl. Acoust.* **2019**, *152*, 73–78. [[CrossRef](#)]
35. Zhou, J.; Asteris, P.G.; Armaghani, D.J.; Pham, B.T. Prediction of ground vibration induced by blasting operations through the use of the Bayesian Network and random forest models. *Soil Dyn. Earthq. Eng.* **2020**, *139*, 106390. [[CrossRef](#)]
36. Nguyen, H.; Bui, X.-N.; Topal, E. Enhancing predictions of blast-induced ground vibration in open-pit mines: Comparing swarm-based optimization algorithms to optimize self-organizing neural networks. *Int. J. Coal Geol.* **2023**, *275*, 104294. [[CrossRef](#)]
37. Zhang, Y.; He, H.; Khandelwal, M.; Du, K.; Zhou, J. Knowledge mapping of research progress in blast-induced ground vibration from 1990 to 2022 using CiteSpace-based scientometric analysis. *Environ. Sci. Pollut. R.* **2023**, *30*, 103534–103555. [[CrossRef](#)] [[PubMed](#)]
38. Nguyen, H.; Bui, X.-N.; Topal, E. Reliability and availability artificial intelligence models for predicting blast-induced ground vibration intensity in open-pit mines to ensure the safety of the surroundings. *Reliab. Eng. Syst. Saf.* **2023**, *231*, 109032. [[CrossRef](#)]
39. Fattahi, H.; Hasanipanah, M. Prediction of Blast-Induced Ground Vibration in a Mine Using Relevance Vector Regression Optimized by Metaheuristic Algorithms. *Nat. Resour. Res.* **2021**, *30*, 1849–1863. [[CrossRef](#)]
40. Qiu, Y.; Zhou, J.; Khandelwal, M.; Yang, H.; Yang, P.; Li, C. Performance evaluation of hybrid WOA-XGBoost, GWO-XGBoost and BO-XGBoost models to predict blast-induced ground vibration. *Eng. Comput.* **2022**, *38*, 4145–4162. [[CrossRef](#)]
41. Chen, W.; Hasanipanah, M.; Nikafshan Rad, H.; Jahed Armaghani, D.; Tahir, M.M. A new design of evolutionary hybrid optimization of SVR model in predicting the blast-induced ground vibration. *Eng. Comput.* **2021**, *37*, 1455–1471. [[CrossRef](#)]
42. Talatahari, S.; Azizi, M. Chaos game optimization: A novel metaheuristic algorithm. *Artif. Intell. Rev.* **2021**, *54*, 917–1004. [[CrossRef](#)]
43. Cambel, A.B. *Applied Chaos Theory: A Paradigm for Complexity*; Elsevier: Amsterdam, The Netherlands, 1993.
44. Fernández-Díaz, A. Overview and Perspectives of Chaos Theory and Its Applications in Economics. *Mathematics* **2023**, *12*, 92. [[CrossRef](#)]
45. Ene, I.-E. Chaos theory, a modern approach of nonlinear dynamic systems. *Rom. J. Inf. Technol. Autom. Control Rev. Română Informatica Și Autom.* **2018**, *28*, 89–96.
46. Yu, Z.; Shi, X.; Zhou, J.; Chen, X.; Qiu, X. Effective assessment of blast-induced ground vibration using an optimized random forest model based on a Harris hawks optimization algorithm. *Appl. Sci.* **2020**, *10*, 1403. [[CrossRef](#)]
47. Shi, X.; Zhou, J.; Li, X. Utilization of a nonlinear support vector machine to predict blasting vibration characteristic parameters in opencast mine. *Prz. Elektrotechniczn* **2010**, *88*, 127–132.
48. Monjezi, M.; Ahmadi, M.; Sheikhan, M.; Bahrami, A.; Salimi, A. Predicting blast-induced ground vibration using various types of neural networks. *Soil Dyn. Earthq. Eng.* **2010**, *30*, 1233–1236. [[CrossRef](#)]
49. Khandelwal, M.; Singh, T. Prediction of blast induced ground vibrations and frequency in opencast mine: A neural network approach. *J. Sound Vib.* **2006**, *289*, 711–725. [[CrossRef](#)]
50. Kumar, R.; Choudhury, D.; Bhargava, K. Determination of blast-induced ground vibration equations for rocks using mechanical and geological properties. *J. Rock Mech. Geotech. Eng.* **2016**, *8*, 341–349. [[CrossRef](#)]
51. Verma, A.K.; Singh, T.N. Intelligent systems for ground vibration measurement: A comparative study. *Eng. Comput.* **2011**, *27*, 225–233. [[CrossRef](#)]
52. Yu, Z.; Shi, X.; Zhou, J.; Gou, Y.; Huo, X.; Zhang, J.; Armaghani, D.J. A new multikernel relevance vector machine based on the HPSOGWO algorithm for predicting and controlling blast-induced ground vibration. *Eng. Comput.* **2022**, *38*, 1905–1920. [[CrossRef](#)]
53. Zhu, C.; Xu, Y.; Wu, Y.; He, M.; Zhu, C.; Meng, Q.; Lin, Y. A hybrid artificial bee colony algorithm and support vector machine for predicting blast-induced ground vibration. *Earthq. Eng. Eng. Vib.* **2022**, *21*, 861–876. [[CrossRef](#)]

54. Zhang, X.; Nguyen, H.; Choi, Y.; Bui, X.N.; Zhou, J. Novel extreme learning machine-multi-verse optimization model for predicting peak particle velocity induced by mine blasting. *Nat. Resour. Res.* **2021**, *30*, 4735–4751. [[CrossRef](#)]
55. Nguyen, H.; Choi, Y.; Monjezi, M.; Van Thieu, N.; Tran, T.-T. Predicting different components of blast-induced ground vibration using earthworm optimisation-based adaptive neuro-fuzzy inference system. *Int. J. Min. Reclam. Environ.* **2024**, *38*, 99–126. [[CrossRef](#)]
56. Tran, Q.-H.; Nguyen, H.; Bui, X.-N. Novel Soft Computing Model for Predicting Blast-Induced Ground Vibration in Open-Pit Mines Based on the Bagging and Sibling of Extra Trees Models. *Comput. Model. Eng. Sci.* **2023**, *134*, 2227–2246. [[CrossRef](#)]
57. Yardimci, A.G.; Erkayaoglu, M. Simulation of blast-induced ground vibrations using a machine learning-assisted mechanical framework. *Environ. Earth Sci.* **2023**, *82*, 508. [[CrossRef](#)]
58. Duvall, W.I.; Fogelson, D.E. *Review of Criteria for Estimating Damage to Residences from Blasting Vibrations*; US Department of the Interior, Bureau of Mines: Winslow, AZ, USA, 1962; Volume 5968.

Disclaimer/Publisher’s Note: The statements, opinions and data contained in all publications are solely those of the individual author(s) and contributor(s) and not of MDPI and/or the editor(s). MDPI and/or the editor(s) disclaim responsibility for any injury to people or property resulting from any ideas, methods, instructions or products referred to in the content.